THE JOURNAL OF PHYSICAL CHEMISTRY B

Article

pubs.acs.org/JPCB

Ultraslow Dynamics at Crystallization of a Room-Temperature Ionic Liquid, 1-Butyl-3-methylimidazolium Bromide

Mamoru Imanari,[†,‡] Kozo Fujii,[†] Takatsugu Endo,[†] Hiroko Seki,[‡] Ken-ichi Tozaki,[§] and Keiko Nishikawa*[,†]

[†]Graduate School of Advanced Integration Science, [‡]Chemical Analysis Center, and [§]Faculty of Education, Chiba University, Chiba 263-8522, Japan

ABSTRACT: We studied the crystallization process of 1-butyl-3-methylimidazolium bromide ([C_4mim]Br) using measurements of supersensitive scanning calorimetry, free induction decay (FID) signals of ^{1}H NMR, and direct observation. These three methods provided consistent, complementary results, which showed extremely slow dynamics at crystallization. This sample does not crystallize during the cooling process, loses mobility, and changes to a coagulated state, which is not the thermodynamic glass state. The FID signals and direct observation in the heating process indicate that the coagulated sample liquefies just before crystallization. The crystallization of [C_4mim]Br does not occur from specialized locations such as the surface or wall of the sample tube but randomly in the liquid. The calorimetric measurements show that it takes 150 min for approximately 3 mg of this sample to crystallize perfectly. Conformational changes of the butyl group continue for approximately 330 min after crystallization. Such slow dynamics are thought to be due to the cooperative linking of crystallization and complex conformational changes in dense fields with high viscosity.

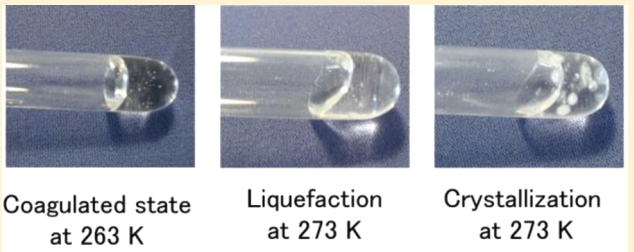

1. INTRODUCTION

Room-temperature ionic liquids (RTILs) constitute a new class of liquids that attract much attention because of their characteristic properties[1−3] and potential utilities as functional liquids.[4−7] Unique properties are remarkably manifested in their thermal behaviors such as low melting point despite being salts, hardness in crystallization, premelting over a wide temperature range, excessive supercooling, and the existence of complex thermal histories.[8−14] In addition, we found peculiar thermal behaviors at the phase changes of imidazolium-based RTILs, namely, "rhythmic melting and crystallization"[15,16] and "intermittent crystallization" in the premelting regions.[16,17] To our knowledge, Holbrey et al.[18] and Hamaguchi et al.[19−21] first demonstrated the existence of plural conformers for constituent ions of RTILs and pointed out its important influence on the thermal properties of RTILs. On the basis of preceding studies of calorimetry combined with Raman spectroscopy, we also attributed most of the above-mentioned unique thermal behaviors of imidazolium-based RTILs to conformational changes and the flexibility of alkyl chains bonding to the imidazolium ring.[14−17,22−25] To elucidate the dynamics at phase changes of RTILs, our recent studies covered measurements of relaxation times by NMR.[26−30]

The present study aims at increasing our understanding of the underlying mechanisms in the phase behaviors of RTILs. In this study, we have focused on the slow dynamics at the crystallization of 1-butyl-3-methylimidazolium bromide ([C_4mim]Br) and have extracted important information from the results of the measurements of supersensitive scanning calorimetry, free induction decay (FID) signals of ^{1}H NMR, and direct observation of the phase change.

2. EXPERIMENTAL SECTION

In general, even a trace amount of water immensely affects the physical and chemical properties of RTILs[31−33] and sometimes hinders the liquids from crystallizing. As [C_4mim]Br is extremely hygroscopic, we paid careful attention to this in the synthesis of the crystalline sample and the preliminary arrangements for the measurements. We synthesized [C_4mim]Br under a dry N_2 atmosphere by mixing doubly distilled *N*-methylimidazole and 1-bromobutane in dry acetonitrile at room temperature. Crystals were obtained by recrystallization of the acetonitrile solution. Then, these crystals were dried for 24 h at 333 K under a vacuum of 10^{-3} Pa and kept under N_2 atmosphere prior to use. The water content was checked using Karl Fischer titration and was measured to be less than 100 ppm. The dried sample was transferred into a pan for the calorimetric measurement or into an NMR sample tube and was then hermetically sealed in a glovebox under a dry N_2 atmosphere.

The scanning calorimeter used in this study was a laboratory-made apparatus, whose basic type has been reported previously.[14,34] Following are the modifications made to the previous differential scanning calorimeter (DSC): (1) usage of

Received: January 21, 2012
Revised: March 10, 2012
Published: March 12, 2012

 © 2012 American Chemical Society dx.doi.org/10.1021/jp300722j | *J. Phys. Chem. B* 2012, 116, 3991−3997

one heat flow sensor (not differential) and (2) attachment of a refrigerator (SC-UD08, Twinbird Co.) for cooling. Peltier modules were utilized for the heat flow sensor and heat pumps, and the system adopted for temperature regulation was a type of predictive controller,[35] instead of a proportional-integral-derivative (PID) controller, to eliminate ripples at on−off switching. For the present setup, the noise level in the heat flow signal was below 7 nW, and the response time was 1 s. This baseline stability, which corresponds to the sensitivity of this calorimeter, is 10^2-10^3 times higher than that of commercially available calorimeters. This apparatus was also designed to scan at a speed within the range 0.01−10 mK/s. The slow scanning speeds such as 0.01 mK/s enabled us to trace very slow thermal phenomena and to mimic a nearly quasi-static process. Because of the short response time, it is possible to trace the dynamics of a thermal process with a relaxation time exceeding 1 s. Measurements can be performed in either direction, heating or cooling, by changing the direction of the electric current through the Peltier modules. This is essential for the thermal measurements of RTILs because many of them often display different behaviors during the cooling and heating processes.

A JEOL-Mu25 pulse NMR instrument with ^{1}H resonance frequency of 25 MHz was used for measuring the relaxation time and FID signals. Because of the choice of the low resonance frequency, we observed that the overall dynamics of the protons in the $[C_4mim]^+$ ions as signal separation by a chemical shift is small. We obtained T_1 values using a 180°−90° inversion recovery pulse sequence. Measurements of T_2 were performed using the $90_x-(180_y-180_y)_n$ Curr−Purcell−Meiboom−Gill pulse sequence for liquid and the solid echo method for solid.[36]

To confirm the outward appearance of the sample in each state, we performed direct observation of $[C_4mim]Br$ in the NMR sample tube by taking photographs. The photographs were taken serially, immediately after removing the sample from the NMR probe provided in the pulse NMR spectrometer.

3. RESULTS AND DISCUSSION

3.1. Calorimetry Data. To understand the present results, we will briefly outline our preceding reports on the phase behaviors of $[C_4mim]Br$ obtained using the laboratory-made DSC with nanowatt stability and sensitivity.[14] When the sample was cooled from the liquid state, we observed no thermal activity in the cooling process even at a very slow scanning rate of 1 mK/s. However, in the heating process, two peaks were found: the exothermic peak for crystallization of the supercooled liquid at approximately 250 K and the endothermic peak for melting at 350 K. Note that the crystallization of the sample occurred in the heating process and not the cooling process. Such a phenomenon is often observed in the phase behaviors of certain ionic liquids.[11,24,25] The crystallization peak of the sample contained two components, and the premelting phenomenon ranged over approximately 10 K.

It has been reported that the *trans*−*trans* (*TT*), *gauche*−*trans* (*GT*), and *gauche*′−*trans* (*G*′*T*) conformers of the butyl group in the $[C_4mim]^+$ ion are stable with a little energy difference among them.[37,38] These three conformations are figured in our previous papers.[24,38] They, in fact, are adopted in many $[C_4mim]$-based ionic liquids and their crystals.[14,15,18−25,39−42] In the case of $[C_4mim]Br$, *TT*, *GT*, and probably *G*′*T* conformers exist in the liquid, supercooled liquid, and glass states,[20−23] while only the *GT* conformation is adopted in the crystalline state.[18] Therefore, both melting and crystallization always occur with structural changes of the conformations of the butyl group. Thus, we concluded that the long-temperature range of premelting and the division of the crystallization peak are caused by cooperative linking of the phase changes and conformational changes in the dense field, where the ions interact closely with each other.[14,22]

In our previous study conducted using the DSC apparatus,[14] it was impossible to cool the sample down to the glass transition temperature (T_g). However, the present NMR measurements and direct observation covered the temperature range of T_g. We performed more calorimetry experiments for a more comprehensive discussion on this topic, especially focusing on crystallization. The differences between the present and previous experimental conditions[14] are as follows. First, in the present study, the sample was cooled to a temperature lower than T_g. Second, because of improvement in the preparation apparatus for removing adventitious water from the sample, the content of water has been greatly decreased down to 100 ppm. It was frequently experienced that some ionic liquids exhibit different phase behaviors depending on their thermal histories. Hence, whether the sample passes through the glass transition is an important factor to stipulate the thermal history of the sample.

In the present calorimetry experiment, the sample (several single crystals of $[C_4mim]Br$) was first heated to 370 K to ensure complete melting. The liquid sample was cooled to 175 K and then heated to 320 K at the same scanning rate of 1 mK/s for both cooling and heating. As shown in Figure 1, no

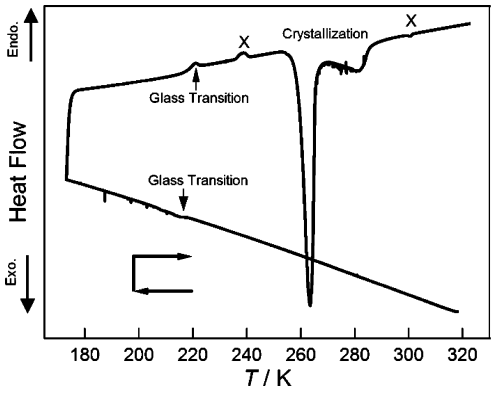

Figure 1. Calorimetry curve of $[C_4mim]Br$ obtained by the laboratory-made calorimeter with sensitivity and stability of 7 nW. Scanning rate for cooling and heating is 1 mK/s. The small peaks denoted by "X" are parasite peaks caused by the thermal activities of the grease.

thermal activity was detected in the cooling process, except for the glass transition at approximately 215 K. On the other hand, in the heating process, the glass transition from glass to supercooled liquid ("coagulated state",[26−28] for details see the next section) was first detected at approximately 220 K. This glass transition temperature (T_g) is in good agreement with the previously reported ones.[43] The small peaks observed at 240 and 300 K are parasite peaks caused by the thermal activities of the grease used for complete thermal contact of the sample pan and the base of the calorimeter.

A large exothermal peak is assigned to crystallization from the coagulated state. The crystallization started at approximately 257 K and continued up to 267 K, which corresponded to 170 min in the present scanning rate. After crystallization, a

dx.doi.org/10.1021/jp300722j | J. Phys. Chem. B 2012, 116, 3991−3997

very broad peak ranging 20 K was observed. This satellite peak is attributed to the annealing of the structural change of the butyl group in $[C_4mim]^+$ ions. Namely, the conformers of *TT* and *G′T*, adopted in the liquid or supercooled liquid state, as well as the *GT* conformer are partially left behind after the crystallization and change gradually to the *GT* conformer that is the only one adopted in the crystal. The broad exothermal peak ranged over 330 min. Similar phenomena (that is, two-step changes) have been found in the phase changes of some RTILs. These phenomena are described as the formation or collapse of the main framework of the crystalline lattice consisting of polar moieties and the following changes of the local domain of a sample or nonpolar moieties with time lag. In other words, the two-step phenomena occur at phase changes of RTILs by the structural formation or collapse of polar and nonpolar moieties. In our DSC experiments of $[C_4mim]Br$ with extremely slow scanning rates such as 0.02 mK/s, the rhythmic melting and crystallization were observed in the premelting region and also in the liquid region just after the perfect melting of the framework of the sample.[15] For the sample of 2.1 mg only, this fluctuation phenomenon continued for approximately 14 h after the melting. For $[i\text{-}C_3mim]Br$, we observed intermittent crystallization in the returning experiment from the premelting region with very slow cooling rate.[16,17] This behavior occurred as the piece-by-piece crystallization of the melting regions left behind in the main crystalline region. Recently, Hamaguchi's group has reported that the conformational change of the butyl group in $[C_4mim]Cl$, at melting, occurs a few seconds after the collapse of the crystalline lattice,[44] which was detected by fast low-frequency Raman spectroscopy.[45] Despite the differences (such as $[C_4mim]Br$, $[C_4mim]Cl$, or $[i\text{-}C_3mim]Br$; and crystallization or melting), the time lag between the main phase change and the following satellite events is thought to be caused by conformational change of ions that always links with the phase change. The time lags of the present crystallization and the melting reported by Hamaguchi's group[44] are different in three digits. It is likely that the conformational change of $[C_4mim]^+$ ions of the former occurs in the solid state, while that of the latter occurs in the liquid state.

Summing up these thermal phenomena, a schematic diagram of Gibbs free energy (G) vs temperature is drawn, as shown in Figure 2. Note that the crystallization of the present sample is not a phase transition but a structural relaxation, and therefore, the crystallization temperature changes are dependent on experimental conditions.

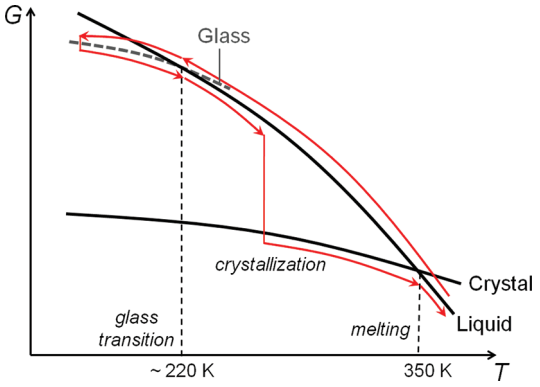

Figure 2. Schematic phase change diagram of $[C_4mim]Br$.

Some spike-like peaks appeared in the glass state in the cooling process and in the satellite peaks in the heating process (Figure 1). The same type of behavior was observed as intermittent crystallization,[16,17] which is not noise as discussed in detail in previous papers.[15−17] The present spike-like peaks are also attributed to the sudden thermal changes of the extremely local areas in the sample, which were left as nonequilibrium states.

3.2. NMR Results. In the preceding study of the NMR measurements of ^1H longitudinal and transverse relaxation times (T_1 and T_2) as a function of temperature, we characterized the coagulated state of $[C_4mim]Br$ and the very slow reorientational molecular motions of the overall $[C_4mim]^+$ ions.[26−28]

First, we mention the coagulated state, which was found for the same sample $[C_4mim]Br$ and described first in our paper.[26] Not limited to the present sample, when a supercooled ionic liquid is cooled, its viscosity becomes much larger, and the movements of constituent ions such as translational motions and some rotational motions are consequently hindered. The supercooled liquid gradually and continuously changes to such a frozen state, although no thermal activity is detected in a DSC or calorimetry experiment. Despite loss of mobility, the state is neither a crystal nor a thermodynamic glass state because the crystal or glass state is characterized in different temperature regions.[43] We named this frozen state the "coagulated state". The temperature range of the gradual change from the supercooled liquid to the coagulated state is 250−260 K. This temperature may be assigned to the critical temperature T_c defined in the mode coupling theory.[46] It is said that T_c is given by approximately $1.2T_g$ for fragile materials such as RTILs. In the present measurement, T_g of this sample is 215−220 K, which agrees with the criterion for T_c. It is known that some physicochemical properties change as the boundary of T_c. In the present sample, the translational motion is frozen in the lower temperature region than T_c (i.e., coagulated state) prior to the thermodynamic glass transition. From a different viewpoint, it is not impossible that this change may belong to the jamming transition.[47]

For the present discussion, our NMR results on $[C_4mim]Br$ are briefly summarized,[28] focusing on its coagulated and crystalline states. Figure 3 shows the traces of $^1H\text{-}T_1$ and $^1H\text{-}T_2$ values as a function of temperature. In the cooling process from the liquid state, the T_1 values (black square) gradually deviate from the simple dipolar relaxation behavior at approximately 260 K after passing through the minimum point. It was

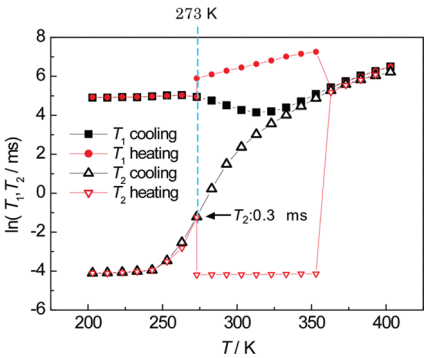

Figure 3. $^1H\text{-}T_1$ and T_2 values of $[C_4mim]Br$ measured as a function of temperature using a ^1H pulse NMR spectrometer.

dx.doi.org/10.1021/jp300722j | J. Phys. Chem. B 2012, 116, 3991−3997

assumed that [C_4mim]Br gradually changed from the supercooled state to the coagulated state at a temperature lower than 260 K. However, [C_4mim]Br did not crystallize in the cooling process, as confirmed by the present calorimetry experiment. The T_2 values (black upward triangles) gradually decrease with lowering temperature and finally reach approximately 17 μs, which is of similar order as that of the crystalline state. In the heating process, the T_1 values (red circles) discontinuously changed at around 273 K because of crystallization. Until this temperature, the T_2 value (red downward triangles) gradually increased to 0.3 ms from 17 μs of the coagulated state, tracing a similar curve as for the cooling process. The increasing T_2 values indicate that the cations become gradually mobile even in the coagulated state as they approach the crystallization point. At the crystallization point, T_2 decreases abruptly and hereafter stays at a constant value of 16−17 μs in the crystalline state ranging from 273 to 350 K.

To reveal the crystallization dynamics from another viewpoint, FID signals of pulse NMR for ^{1}H were observed in this study. An FID signal is a transverse component of magnetization which appears just after applying the excitation pulse. If the excitation pulse is applied along the x axis, the transverse magnetization at $t = 0$, $M_y(0) = M_0$, appears along the y axis, where M_0 is an equilibrium magnetization in the z axis. The transverse magnetization freely decays to the equilibrium state of zero. The transverse magnetization after t, $M_y(t)$, can be expressed as follows[36]

$$M_y(t) = M_0 \exp(-t/T_2)$$

We first focused on the precrystallization of [C_4mim]Br. The FID signals from 223 to 263 K (heating process) are shown in Figure 4. It is clear that the decay signal becomes slower as the crystallization point (273 K) is approached and that this change occurs abruptly from temperatures that are 20 K lower than the crystallization point. These changes in the decay speed show that the cations in the coagulated state are mobilized gradually but slightly as the temperature rises and become abruptly mobile at temperatures that are 20 K lower than the crystallization point. This offers a possible explanation for the crystallization peak that ranges over a wide temperature region that was found in the calorimetric measurements (Figure 1). This broad peak probably corresponds to this dynamical change in cations. From the Fourier transform of a FID curve, an NMR spectrum and then the corresponding T_2 value are obtained. The temperature-dependent change of the FID curves corresponds to the change of T_2 values shown by red triangles in the range of 223−273 K in Figure 3.

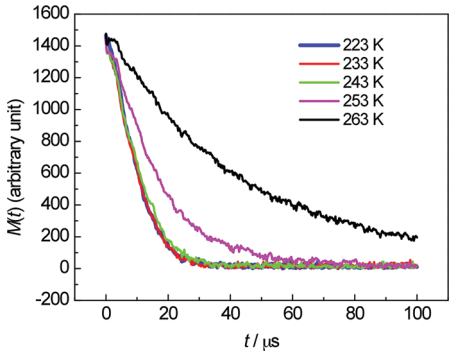

Figure 4. Free induction decay (FID) signals of pulse ^{1}H NMR from 223 to 263 K (heating process).

Next, we obtained the time dependence of FID signals, fixing the sample temperature at the crystallization point of 273 K. In general, the FID signal of a solid sample decays in lesser than a millisecond, while that of a liquid sample decays within a few seconds. If the sample consists of two components (denoted by "**1**" and "**2**") with different transverse relaxation times of $T_{2,1}$ and $T_{2,2}$, respectively, the FID signal is expressed as follows

$$M_y(t) = M_1 \exp(-t/T_{2,1}) + M_2 \exp(-t/T_{2,2})$$

where M_1 and M_2 are weights of components **1** and **2**, respectively. When the difference between $T_{2,1}$ and $T_{2,2}$ is large like the combination of solid and liquid, we can easily separate the two components. Moreover, as shown in the present calorimetry experiment, the crystallization of [C_4mim]Br is very slow in such that it takes more than several to ten minutes. Therefore, the slow crystallization can be easily monitored by the FID signals of pulse NMR.

Keeping the sample at the crystallization temperature (273 K), the FID signals were acquired in a 4 min period. The results using a sample tube of 9 mm in inner diameter are shown in Figure 5. In the crystallization of [C_4mim]Br at 273 K, at first, a FID signal with only a long-decay component (#1 and #2, red and orange curves, respectively) appears, and then 10 min later, another small FID component with a very short decay time appears at the early region in the FID signal (#3 green curve). This short FID component gradually increases over time (from #3 green to #7 dark blue curves). Finally, the FID signal is composed only of the component with short decay time (#8 black line) at approximately 30 min after setting the temperature at 273 K.

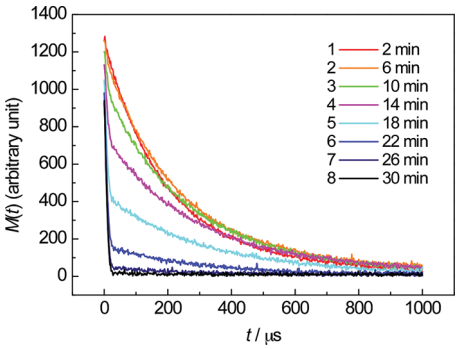

Figure 5. Time dependence of FID signals, fixing temperature at the crystallization point of 273 K.

The FID signals with long and short decay times correspond to the liquid and crystal components, respectively. The ratios of crystal and liquid components can be estimated by decomposing each FID signal into two. The results are shown in Figure 6(a). The ratio curve of crystallization is separated into three stages. In the first stage for the range of 0−14 min, we could not obtain the detailed data because the crystallization component in the FID signal was very little as shown in Figure 5. In this stage, the nuclear formation of crystal is thought to occur. In the second stage for the range of 16−44 min, the crystal component linearly increases with time. First, we had expected higher power dependence on elapsed time in crystallization, forecasting that crystallization would occur on the surface of once-generated crystal grains. This unexpected

dx.doi.org/10.1021/jp300722j | J. Phys. Chem. B 2012, 116, 3991−3997

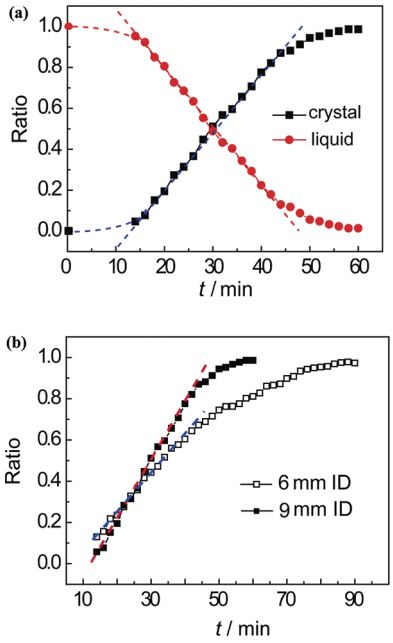

Figure 6. (a) Time dependence of the ratio of crystal and liquid moieties at the crystallization temperature of 273 K. (b) Comparison of the ratio curves of crystallization using different sample tubes. The closed and open squares are the data with the sample tubes of 9 and 6 mm in inner diameter.

growth may be related to the fact that the crystallization of the present sample is linked with the conformational change of $[C_4mim]^+$ ions.[14,22] The speed of the conformational change may be constant independent of the elapsed time. It is thought that the saturation in the later time (the third stage) is because $[C_4mim]Br$ crystallizes in the limited space of the NMR sample tube. The wall of the tube may prevent the inherent growth of the crystal.

To check the effect of wall of the sample tube, we acquired the ratio curves of crystallization using different sample tubes. In Figure 6(b), the closed and open squares are the data with the sample tubes of 9 and 6 mm in inner diameter, respectively. The sample amount for the 6 mm tube is about 0.6 times the one for the 9 mm tube. In spite of the smaller quantity, it takes longer time for the sample to crystallize perfectly. As shown in Figure 6(b), the third stage for the 6 mm tube starts earlier. This result indicates that the wall of the sample tube works as an inhibitor of growth of crystal. In the second stage for the 6 mm tube, the crystal component also increases linearly with time. It is noted that the slope ratio of the lines is nearly 3:2, surprisingly corresponding to the ratio of 9:6 in inner diameter of the sample tube.

We assume that the crystallization mechanism is much more complex than the usual crystallization of the arrangement of simple ions around crystalline nucleuses. Although we are yet to find the complete explanation for this behavior, the linear dependence provides some information on the crystallization mechanism of the sample. To study details of the nuclear formation process, other experiments that are sensitive for very little quantity of crystal may be desired.

The present FID experiments on $[C_4mim]Br$ reveal three points. First, the softening of the sample occurs just before crystallization from the coagulated state. Second, the crystallization of $[C_4mim]Br$ proceeds by very slow dynamics, and its process is affected by the surroundings such as wall of the sample tube. Third, the growth of crystal is linearly dependent on elapsed time at the crystallization temperature.

3.3. Direct Observation. Figure 7 shows the photographs of $[C_4mim]Br$ at different temperatures in the NMR sample

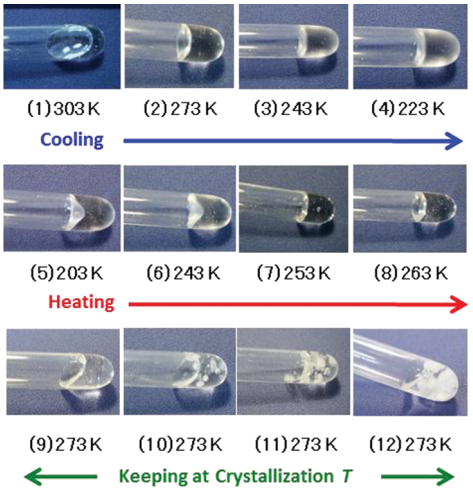

Figure 7. Photographs of $[C_4mim]Br$ at decisive temperatures. Photos (1)−(4) (first row) and Photos (5)−(8) (second row) correspond to the cooling process and heating process, respectively. Photos (9)−(12) (third row) were taken over time, keeping the sample at the crystallization temperature of 273 K.

tube. Photos (1)−(4) (first row) were taken in the cooling process. Photo (1), which was taken at 303 K, refers to the supercooled liquid state, where the sample displays fluidity (T_2: 10.6 ms). Photos (2)−(4) correspond to a variant of the supercooled liquid state, where the sample does not display fluidity. This state was named the coagulated state.[26] The T_2 values of ^1H NMR for these states (Photos (2)−(4)) are 17−18 μs, as described in Section 3.2.

The glass transition in the cooling process probably occurred between the shots taken for Photos (4) and (5), considering that the signal of the glass transition appeared at approximately 215 K in the calorimetry experiment (Figure 1). As shown in Photo (5) at 203 K, a hollow at the center of the sample surface was observed, which was probably formed at the glass transition. This hollow suggests a reduction in sample volume at the glass transition in the cooling process. While there was no signal in the T_1 and T_2 values of NMR for the transition from the coagulated state to the glass state (Figure 3), we detected the phase change by this direct observation (volume change), as well as by the calorimetric measurement (Figure 1).

Photos (5)−(8) (second row) were taken in the heating process at temperatures ranging from 203 to 263 K. In this region, the sample did not show fluidity. The hollow on the sample surface was observed up to 243 K, although the glass transition in the heating process (approximately 220 K in the calorimetry experiment, see Figure 1) had already occurred. Therefore, in the heating process, the large volume change did not occur at the glass transition, but later. The hollow disappeared at approximately 253 K. This temperature corresponds to the one at which the T_2 value abruptly increases from the smaller value of 17−18 μs (Figure 3). This volume expansion seems to give the ions a little mobility.

Photos (9)−(12) (third row) were taken over a time range while keeping the sample at the crystallization temperature of 273 K. Initially, the sample exhibited fluidity (T_2: 0.3 ms), as

dx.doi.org/10.1021/jp300722j | J. Phys. Chem. B 2012, 116, 3991−3997

shown by Photo (9), and then started to randomly crystallize in the liquid (Photos (10)−(12)). On the basis of this, the following two points are observed. First, it appears that for the crystallization of [C_4mim]Br fluidity is necessary. This is because *TT*, *GT*, and *G′T* conformers of the butyl group coexist in the coagulated state of [C_4mim]Br,[20−23] while only *GT* conformation is adopted in the crystalline state.[14] The coagulated state must loosen for cations to get mobility and to change their conformations. This is observed as the liquefication just before the crystallization from the coagulated state. Second, the crystallization of [C_4mim]Br occurs not from specialized locations such as the surface or wall of the sample tube but randomly in the liquid.

4. CONCLUDING REMARKS

We investigated the ultraslow crystallization of [C_4mim]Br using calorimetric measurements, FID measurements of ^{1}H NMR, and direct observation. These three methods provide consistent, complementary results. Overall, the crystallization of the sample is extremely slow and complex. This sample does not crystallize in the cooling process, loses its mobility, and changes to a coagulated state prior to the glass transition. In the heating process, the coagulated sample liquefies just before crystallization. It takes several tens of minutes for a sample of approximately 3 mg to crystallize. Conformational changes of the butyl group seem to follow after the crystallization of polar moieties; namely, the former are detected as the broad peak in the calorimetry curve ranging 20 K in temperature or 330 min in time.

Slow dynamics, characteristic of ionic liquids, and anomalous phenomena induced from them have attracted much attention. As a result, theoretical[48−50] as well as experimental studies[14−17,22−28,51,52] are currently in progress. Limited to their phase behaviors because the numerous ion pairs, such as 10^{12}−10^{15} pairs, interact with each other and move cooperatively,[15−17] the dynamics at phase changes are frequently slow enough to be detected directly. For example, through the measurement of viscoelastic moduli, McKenna's group found a slow aging phenomenon ranging over several days close to the glass transition temperature for certain ionic liquids including [C_4mim]PF_6.[53] In addition, Hamaguchi's group has reported the time lag of conformational change in the butyl group and the collapse of crystalline lattice for the melting of [C_4mim]-Cl.[44] Our present investigation on [C_4mim]Br also exhibits one of the unique phase behaviors of RTILs. Similarly, the phase behaviors of many RTILs are governed by slow dynamics and can be observed as unique and anomalous phenomena at phase changes. Such slow dynamics are due to the correlation of phase changes and complex conformation changes in dense fields with high viscosity. It is reported that, due to the Coulomb interaction of constituent cations and anions, the density of an ionic liquid is 1.2−1.3 times higher than the mixtures of molecular liquids with similar components.[54]

As mentioned above, the slow dynamics at the phase changes of several ionic liquids have been frequently observed and reported. The present study may be the first report on slow and curious dynamics in the phase behaviors that is systematically approached from various angles. Especially, the liquefaction in the heating process between the frozen state and crystalline one may be the first observation in ionic liquids.

AUTHOR INFORMATION

Corresponding Author

*E-mail: k.nishikawa@faculty.chiba-u.jp.

Notes

The authors declare no competing financial interest.

ACKNOWLEDGMENTS

The present study was partially supported by the Ministry of Education, Culture, Sports, Science and Technology (MEXT) of Japan (No. 17073002: Grant-in-Aids for Scientific Research in Priority Area "Science of Ionic Liquids", and No. 21245003: Grant-in-Aids for Scientific Research (A)).

REFERENCES

(1) Physical Chemistry of Ionic Liquids; Wishart, J. F., Castner, E. W., Jr., Eds. The special issue of *J. Phys. Chem. B* **2007**, *111*, No. 18.
(2) Ionic Liquids; Rogers R. D., Voth, G. A., Eds.; The special issue of *Acc. Chem. Res.* **2007**, *40*, No.11.
(3) Wishart, J. F.; Castner, E. W., Jr. *J. Chem. Phys.* **2010**, *132*, No. 120901.
(4) *Electrochemical Aspects of Ionic Liquids*; Ohno, H., Ed.; John Wiley: Hoboken, 2005.
(5) Angell, C. A.; Byrne, N.; Belieres, J. *Acc. Chem. Res.* **2007**, *40*, 1228−1236.
(6) Plechkova, N. V.; Seddon, K. R. *Chem. Soc. Rev.* **2008**, *37*, 123−150.
(7) Greaves, T. L.; Drummond, C. J. *Chem. Rev.* **2008**, *108*, 206−237.
(8) Holbray, J. D.; Seddon, K. R. *J. Chem. Soc., Dalton Trans.* **1999**, *13*, 2133−2139.
(9) Ngo, H. L.; LeCompte, K.; Hargens, L.; McEwen, A. B. *Thermochim. Acta* **2000**, *357*, 97−102.
(10) Huddleston, J. G.; Visser, A. E.; Reichert, W. M.; Willauer, H. D.; Broker, G. A.; Rogers, R. D. *Green Chem.* **2001**, *3*, 156−164.
(11) Fredlake, C. P.; Crosthwaite, J. M.; Heert, D. G.; Aki, S. N. V.; Brennecke, J. F. *J. Chem. Eng. Data* **2004**, *49*, 954−964.
(12) Marsh, K. N.; Boxall, J. A.; Lichtenthaler, R. *Fluid Phase Equilib.* **2004**, *219*, 93−98.
(13) Nishida, T.; Tashiro, Y.; Yamamoto, M. *J. Fluorine Chem.* **2003**, *120*, 135−141.
(14) Nishikawa, K.; Wang, S.; Katayanagi, H.; Hayashi, S.; Hamaguchi, H.; Koga, Y.; Tozaki, K. *J. Phys. Chem. B* **2007**, *111*, 4894−4900.
(15) Nishikawa, K.; Wang, S.; Tozaki, K. *Chem. Phys. Lett.* **2008**, *458*, 88−91.
(16) Nishikawa, K.; Wang, S.; Endo, T.; Tozaki, K. *Bull. Chem. Soc. Jpn.* **2009**, *82*, 806−812.
(17) Nishikawa, K.; Tozaki, K. *Chem. Phys. Lett.* **2008**, *463*, 369−372.
(18) Holbrey, J. D.; Reichert, W. M.; Nieuwenhuyzen, M.; Johnston, S.; Seddon, K. R.; Rogers, R. D. *Chem. Commun.* **2003**, 1636−1637.
(19) Hayashi, S.; Ozawa, R.; Hamaguchi, H. *Chem. Lett.* **2003**, *32*, 498−499.
(20) Ozawa, R.; Hayashi, S.; Saha, S.; Kobayashi, A.; Hamaguchi., H. *Chem. Lett.* **2003**, *32*, 948−949.
(21) Hamaguchi, H.; Ozawa, R. *Adv. Chem. Phys.* **2005**, *131*, 85−104.
(22) Endo, T.; Tozaki, K.; Masaki, T.; Nishikawa, K. *Jpn. J. Appl. Phys.* **2008**, *47*, 1775−1779.
(23) Endo, T.; Nishikawa, K. *J. Phys. Chem. A* **2008**, *112*, 7543−7550.
(24) Endo, T.; Kato, T.; Tozaki, K.; Nishikawa, K. *J. Phys. Chem. B* **2010**, *114*, 407−411.
(25) Endo, T.; Kato, T.; Nishikawa, K. *J. Phys. Chem. B* **2010**, *114*, 9201−9208.
(26) Imanari, M.; Nakakoshi, M.; Seki, H.; Nishikawa, K. *Chem. Phys. Lett.* **2008**, *459*, 89−93.
(27) Imanari, M.; Tsuchiya, H.; Seki, H.; Nishikawa, K.; Tashiro, M. *Magn. Reson. Chem.* **2009**, *47*, 67−70.
(28) Imanari, M.; Uchida, K.; Miyano, K.; Seki, H.; Nishikawa, K. *Phys. Chem. Chem. Phys.* **2010**, *12*, 2959−2967.

(29) Endo, T.; Imanari, M.; Seki, H.; Nishikawa, K. *J. Phys. Chem. A* **2011**, *115*, 2999−3005.
(30) Endo, T.; Widgeon, S.; Yu, P.; Sen, S.; Nishikawa, K. *Phys. Rev. B* **2012**, *85*, 054307−1−9.
(31) O'Mahony, A. M.; Silvester, D. S.; Aldous, L.; Hardacre, C.; Compton, R. G. *J. Chem. Eng. Data* **2008**, *53*, 2884−2891.
(32) Hang, S.; Li, X.; Chen, H.; Wang, J.; Zhang, J.; Zhang, M. *J. Chem. Eng. Data* **2004**, *49*, 760−764.
(33) Ries, L. A. S.; Amaral, F. A.; Matos, K.; Martini, E. M. A.; Souza, M. O.; Souza, R. F. *Polyhedron* **2008**, *27*, 3287−3293.
(34) Wang, S.; Tozaki, K.; Hayashi, H.; Inaba, H. *J. Therm. Anal. Calorim.* **2005**, *79*, 605−613.
(35) Kojima, A.; Yoshimura, Y.; Iwasaki, H.; Tozaki, K. in: Ripple, D.C. (Ed.) Temperature: Its Measurement and Control in Science and Industry, Vol. 7, *AIP Conference Proceedings*, American Institute of Physics, 2003, Vol. *684*.
(36) Farrar, T. C.; Becker, E. D. *Pulsed and Fourier Transform NMR*; Academic Press: New York, 1971.
(37) Turner, E. A.; Pye, C. C.; Singer, R. D. *J. Phys. Chem. A* **2003**, *107*, 2277−2288.
(38) Tsuzuki, S.; Arai, A. A.; Nishikawa, K. *J. Phys. Chem. B* **2008**, *112*, 7739−7747.
(39) Berg, R. W. *Monatsh. Chem.* **2007**, *138*, 1045−1075 and references cited therein..
(40) Triolo, A.; Mandanici, A.; Russina, O.; Rodriguez-Mora, V.; Cutroni, M.; Hardacre, C.; Nieuwenhuyzen, M.; Bleif, H.-J.; Keller, L.; Ramos, M. A. *J. Phys. Chem. B* **2006**, *110*, 21357−21364.
(41) Saha, S.; Hayashi, S.; Kobayashi, A.; Hamaguchi, H. *Chem. Lett.* **2003**, *32*, 740−741.
(42) Nakakoshi, M.; Shiro, M.; Fujimoto, T.; Machinami, T.; Seki, H.; Tashiro, M.; Nishikawa, K. *Chem. Lett.* **2006**, *35*, 1400−1401.
(43) Paulechka, Y. U.; Kabo, G. J.; Blokhin, A. V.; Shaplov, A. S.; Lozinskaya, E. I.; Vygodskii, Y. S. *J. Chem. Thermodyn.* **2007**, *39*, 158−166.
(44) Okajima, H.; Hamaguchi, H. *Chem. Lett.* **2011**, *40*, 1308−1309.
(45) Okajima, H.; Hamaguchi, H. *Appl. Spectrosc.* **2009**, *63*, 958−960.
(46) Das, S. P. *Rev. Mod. Phys.* **2004**, *74*, 785−851.
(47) Biroli, G. *Nat. Phys.* **2007**, *3*, 222−223.
(48) Hu, Z.; Margulis, C. J. *Acc. Chem. Res.* **2007**, *40*, 1097−1105.
(49) Maginn, E. J. *Acc. Chem. Res.* **2007**, *40*, 1200−1207.
(50) Roy, D.; Patel, N.; Conte, S.; Maroncelli, M. *J. Phys. Chem. B* **2010**, *114*, 8410−8424.
(51) Saito, M.; Seto, M.; Kitao, S.; Kobayashi, Y.; Higashitaniguchi, S.; Kurokuzu, M.; Sugiyama, M.; Yoda, Y. *Appl. Phys. Express*, **2009**, *2*, No. 026502.
(52) Kakiuchi, T.; Yasui, Y.; Kitazume, Y.; Nishi, N. *ChemPhysChem* **2010**, *11*, 2912−2918.
(53) Shamin, N.; McKenna, G. B. *J. Phys. Chem. B* **2010**, *114*, 15942−15952.
(54) Shirota, H.; Castner, E. W. *J. Phys. Chem. A* **2005**, *109*, 9388−9392.